ADDITIVE MANUFACTURING OF FLAME-RETARDANT POLYAMIDE 6 NANOCOMPOSITES VIA FUSED FILAMENT FABRICATION (FFF)

Hao Wu[1], Abdullah Kafi[2], Haewon Kim[1,3], Rishabh Shah[3], Stuart Bateman[2], Joseph H. Koo[1,3]

[1]KAI, LLC, Austin TX. USA

[2]School of Engineering, RMIT University, Melbourne, VIC, Australia.

[3]Walker Department of Mechanical Engineering, The University of Texas at Austin, Austin TX. USA.

ABSTRACT

Additive manufacturing has been under rapid development over the past decade. Even so, the range of available materials to produce functional parts using additive manufacturing techniques remain limited. In this study, a flame-retardant (FR) nanocomposite polyamide 6 (PA6) formulation was compounded and extruded into Fused Filament Fabrication (FFF) compatible filaments. Materials properties were characterized before printing. The FR PA6 nanocomposite showed lower MFI than the unmodified PA6 as expected, however the FR PA6 formulation exhibited improved thermal stability at high temperatures and more importantly significantly reduced flammability. To examine the printability of this FR PA6 nanocomposite formulation, the extruded filaments were printed using FFF. The print quality was optimized by fine tuning various printing parameters.

1. INTRODUCTION

Additive manufacturing (AM) is a process of joining or solidifying materials layer upon layer to make parts directly from a 3D digital models [1]. The technique has attracted tremendous research attention from both academia and industry [2]. With AM, topologically optimized and otherwise difficult to manufacture designs can be printed without the need for tooling. This allows the manufacture of lightweight integrated structures which is of interest to a range of industries including the transportation sector to assist in reducing fuel burn and hence emissions. In the medical industry, AM made customization of medical devices faster and more affordable [3]. For automotive manufacturers, AM could save cost by improving lead time for manufacturing of low volume customized parts. Among the various AM techniques, material extrusion 3D printing (ME3DP), also commonly known as fused filament fabrication (FFF) or Fused Deposition Modelling (FDM) is currently the most widely available AM platform. As illustrated in Fig. 1, FFF machines have nozzles that melt and extrude the thermoplastic filament allowing layer by layer addition of molten polymer. The build platform is usually heated above room temperature to reduce wrapping and support materials are used to provide scaffolding to support overhang structures or internal cavities [4]. Advantages of FFF include the relative ease of use, materials handling and availability of a range of printers at different price points. One

Copyright 2019. Used by the Society of the Advancement of Material and Process Engineering with permission.

SAMPE Conference Proceedings. Charlotte, NC, May 20-23, 2019. Society for the Advancement of Material and Process Engineering – North America.

well known limitation for FFF, however, is the limited range of materials available for selection. By far, the majority of the materials currently used for FFF are commodity thermoplastics such as ABS and PLA [5]. Although ultra-performance inherently FR polymers such as polyether imides (like SABIC's ULTEM) have been commercialized for 3D printing, their high cost and complexity through high melt temperature is often prohibitive leading to few flame-retardant material choices available. The development of FR engineering materials with good mechanical properties at low cost will help to expand the applicability of FFF in aerospace, automotive and construction industries.

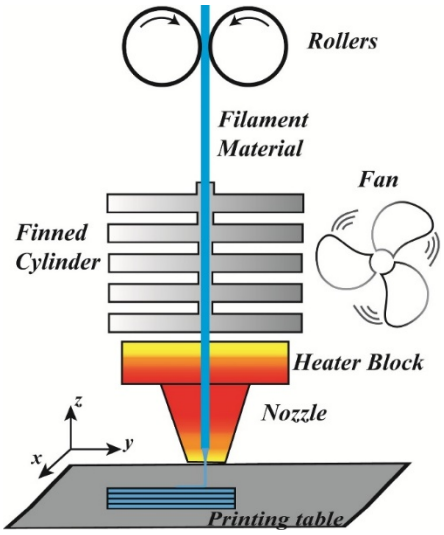


Figure 1 Illustration of FFF setup [6].

Polyamide 6 or nylon 6 is an engineering thermoplastic with high strength and low cost. Unfortunately nylon 6 and many other engineering polymers are highly flammable which limits their application. To overcome this drawback, flame retardant additives are compounded into nylon 6 commercially to produce grades with reduced flammability. Traditional flame retardants, such as halogenated flame retardants are widely used but halogens are considered as a hazardous species and questionable in future use [7]. As a result, non-halogenated flame retardant has been developed. Among them, phosphorous-based flame retardants are found to be very effective in oxygen containing polymers, such as polyamides and polyesters [8]. Over the past few decades, various studies have shown that nanoparticles, such as nanoclay and carbon nanotubes could provide synergistic effect when combined with intumescent flame retardants [9, 10].

One often neglected problem associated with flame-retardant polymers created by incorporating additives is that they usually experience a significant loss in mechanical properties[11]. For example, nylon 6 blended with non-halogenated FR fillers was shown to achieve self-extinguishing and non-drip behavior but the FR blend exhibited a dramatic reduction in ductility. Previous studies from our research group developed a FR nylon 6 formulation with improved ductility by using thermoplastic elastomer and nanoclay additives [10, 12-16]. Detailed discussion about the formulations can be found in [16]. A prospective formulation incorporated three components into the FR nylon 6 formulation, including a non-halogenated intumescent

flame-retardant additive, a SEBS grafted thermoplastic elastomer, and a montmorillonite (MMT) organo-nanoclay. The optimum formulation with balanced FR and mechanical performances was chosen for this current study was composed of 75 wt.% nylon 6, 15 wt.% flame retardant additive, 5 wt.% nanoclay, and 5 wt.% elastomer.

Following the initial study [4], the goal of this study is to investigate the processability of the FR nylon 6 formulation for FFF application. First, the materials need to be compounded and extruded into filaments so that it not only meets the requirements of FFF capabilities but also achieves good dispersion of additives especially the nanoparticles. After filament extrusion, test specimens were fabricated using FFF and finally CT scan were performed to examine the print quality.

2. EXPERIMENTATION

2.1 Materials

Low viscosity non-lubricated nylon 6 (density of 1.13 g/cm^3), was obtained from Honeywell, Inc. and dried at 80°C for 24 hours prior to processing. Flame-retardant additive was provided by Clariant International Ltd. Its flame-retardant mechanism is through intumescence, whereby a protective foam is formed to isolate heat and oxygen from the combustion fuel source [17, 18]. The SEBS elastomer has been shown to have good compatibility with nylon 6 even without high shear mixing [19]. Organically modified Montmorillonite (MMT) organoclay was provided by Southern Clay Products. Nylon 6 pellets were dried overnight at 80°C before processing while flame retardant, elastomer, and nanoclay were used as received.

2.2 Processing

2.2.1 Compounding and filament extrusion

Filaments were processed using a Process 11 parallel co-rotating twin screw extruder from Thermo-Scientific Inc. The co-rotating twin screw extruder provides high shear mixing which ensures adequate dispersion of the organo-clay. Materials were melted and mixed at 240ºC, with a screw speed of 100 rpm. To ensure a homogenous dispersion, formulations with varying concentrations were pre-mixed prior to melt compounding. Melt extrudate were drawn through a custom-made water bath before being collected onto the spool attached to the filament winder (Figure 1).

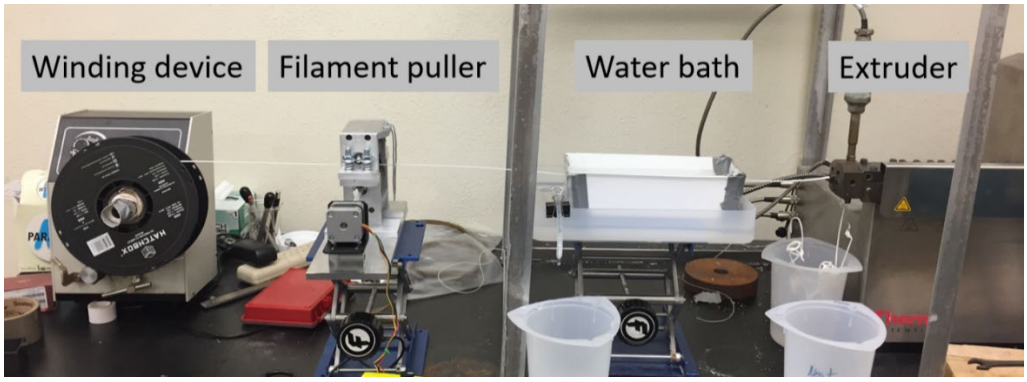


Figure 2 Filament Extrusion set up.

2.2.2 FFF Printing

To examine the material printability, 20 mm square shape cubes of FR PA6 nanocomposite formulation were printed using a Roboze one+400 manufactured by Roboze S.P.A. (Bari, Italy) based on following printer settings:

- Infill: 100%
- Infill Pattern: Rectilinear
- Raster Angle: 0-90
- Hotend Temperature: 240℃
- Bed Temperature: 110℃
- Print Speed: 30-50 mm/min

In order to prevent warpage which causes delamination of deposited polymers from the bed, several commercially available bed films were investigated in addition to various print speeds. None of traditional paper film (AB 003 & 006) for Nylon was shown to be suitable except the combination of PEI film and hair spray (HS). Selection of the right film and a slow print speed offered the least visual delamination of the build from the build platform.
Extrusion multiplier (EM) was optimized in this study to achieve the best surface finish and homogeneity in printed cubes. EM was controlled by changing the multiplier option in simplify3D. Print speed also slowed down from 50 to 30 mm/min to prevent early print failure. Once the right film and HS combination was found as shown in Table 1, the next step was to increase the multiplier from 0.95 to 1.05 until there was no holes in upper cube surface.

Table 1 FR PA6 Optimization parameters and consequences

Print RUN	Extrusion Multiplier	Film	LAYER H.	Warpage	Consequence
1ST RUN	0.95	AB-003	0.20	Y	Delamination (100%)
2ND RUN	0.95	AB-006	0.20	Y	Delamination (100%)
3RD RUN	0.95	AB006 (PE Finish)	0.20	Y	Delamination (100%)
4TH RUN	0.95	PE	0.20	Y	Delamination (100%)
5TH RUN	0.95	PE-HS	0.12	N	Delamination (10%)
6TH RUN	0.98	PE-HS	0.12	N	Delamination (10%)
7TH RUN	1	PE-HS	0.12	N	Delamination (10%)
8TH RUN	1.05	PE-HS	0.12	N	Delamination (10%)

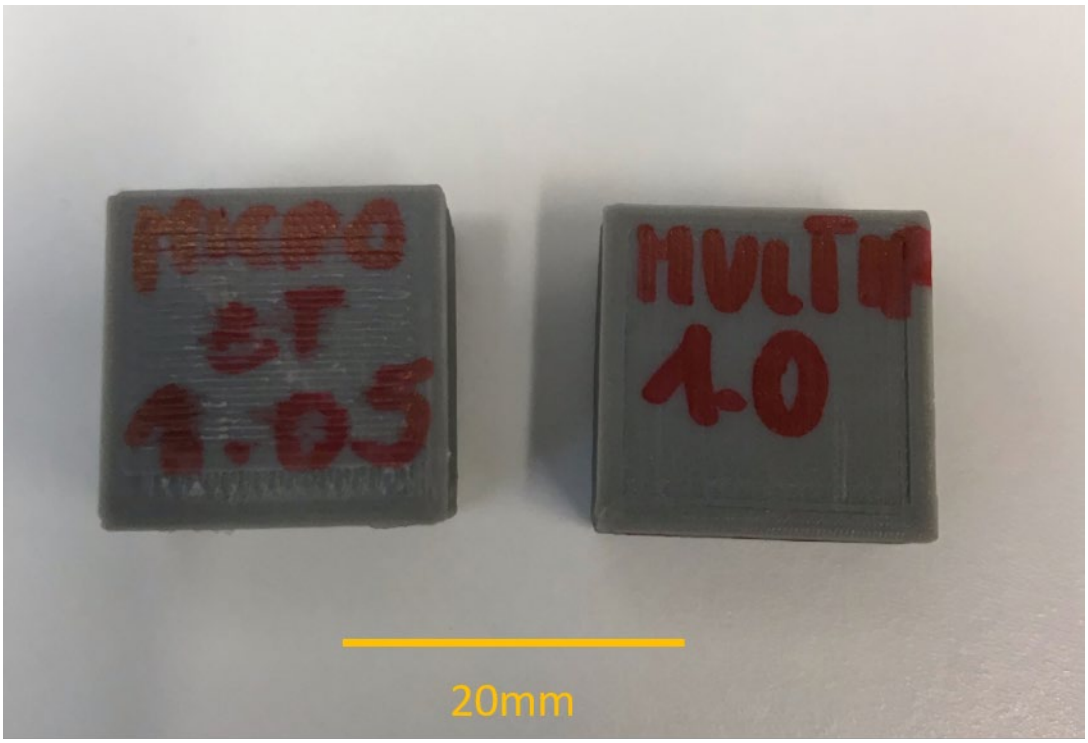


Figure 3 Effect of Extrusion Multiplier on PA6 surface finish (Top surface). Left Cube was printed at Multiplier 1.05 and the Right Cube at Multiplier 1.0 whereas 1.0 achieved the best surface without any lines or grooves.

2.3 Characterization

2.3.1 Melt flow index

A Dynisco LMI 4000 series Melt Indexer (Franklin, MA, USA) with an applied weight of 2060 g was used for the MFI test in accordance with ASTM D1238. All materials were conditioned at 25 ℃ and 50% RH for 48 hours before testing. The barrel temperature was kept at 240 ºC for both neat PA6 and the FR PA6 nanocomposite. For each test, about 5 g of materials were kept in the heated barrel for 180 s before extruding. To ensure test accuracy, a total of 5 tests were performed on each sample and the average and error bars were calculated.

2.3.2 TGA

Thermal decomposition onset of each polymer blend was assessed using a TGA-50 from Shimadzu Scientific Instruments. Samples with size between 15-20 mg were heated in a nitrogen environment from room temperature to 1,000 °C at a heating rate of 10 °C/min. The nitrogen flow was 20 mL/min. Single TGA test was performed on each formulation and was used to determine the decomposition temperatures at 10% mass loss ($T_{10\%}$). The char yield is defined as the weight percentage at 1,000 °C.

2.3.3 MCC

A Micro-scale Combustion Calorimeter (MCC2, Govmark, Inc.) was used to measure the thermal combustion properties according to ASTM D7309-2007. The combustor temperature was held constant at 900 °C and the heating rate of the pyrolysis was 1 °C/s. The percentage of

oxygen consumption was measured to calculate the corresponding heat release. All values reported in the discussion are average of 3 tests, stand errors are also reported.

2.3.4 Micro-CT scan

Stage 1. Scanning the samples

Scans were performed using a Bruker Skyscan 1275 operating at 30 kV 100 µA with no filter in place. The object was placed on a brass sample stage and positioned to achieve an image pixel size. The height was adjusted to image the thickest part of the sample. Samples were scanned with the following settings: 0.4° rotation step, 360° scanning, 4 frame averaging, total of 901 shadow projections (raw images). Camera settings were: 1944x1536 resolution, 67 ms exposure.

Stage 2. Reconstruction

Program NRecon is used to calculate cross sections from the raw images with the following software determined post processing corrections: Smoothing, Misalignment compensation, Ring artifacts reduction, Beam-hardening correction (constant at 30% across all samples). The dynamic image range was set from 0.0 to 0.0170 for all samples.

In order to analyze the volume inside the object, a rectangular shape ROI was set. The ROI (red rectangle) was created over a 2D slice and applies to all slices. Each slice was checked to make sure the ROI stays within the object. Adjustments to the ROI was made when necessary. Below snapshot was taken from NRecon software window where the raw data (shadow projection) and a reconstructed slice is shown.

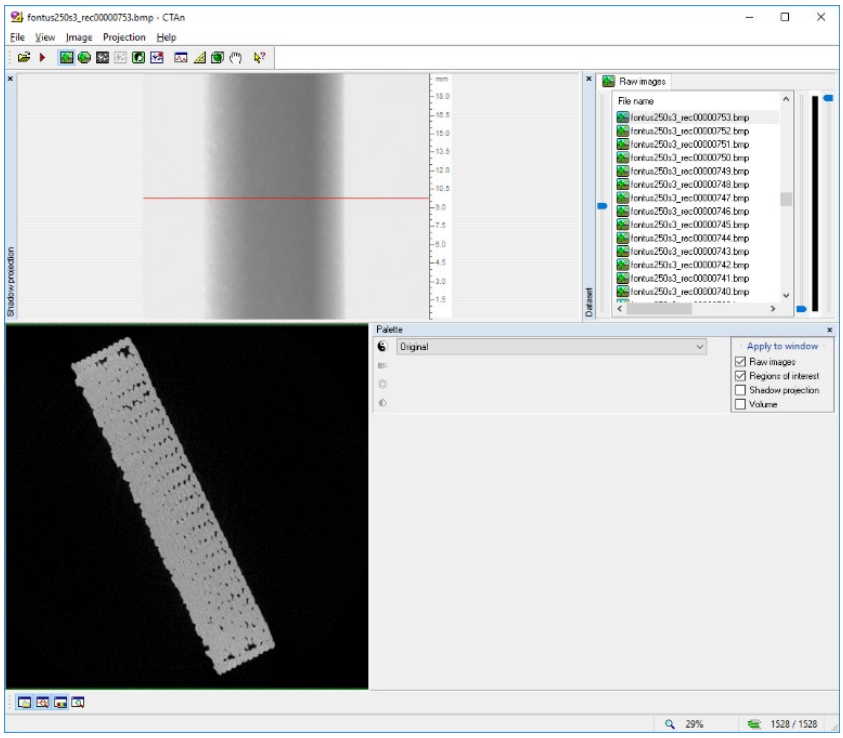


Figure 4 Stage 3. Analysis of images using CTan.0

Software CTan is used to binarize images in order to segregate areas of different density. Cross sections are represented as a binary image of material (1) and air (0). Porosity was calculated from the binarized images. In stage 3 (CTan), binarized images were exported as a model file.

3. RESULTS

3.1 Melt flow index

The melt flow index (MFI) of both neat PA6 and the FR PA6 nanocomposite tested at 240°C are shown in Figure 4. Neat PA6 has an MFI of 21.5 g/10 min, which significantly higher than its FR nanocomposite at 6.8 g/10 min. The increased viscosity of the FR PA6 nanocomposite was caused by the restricted chain movement induced by formation of a nano-filler network [20]. It was noted, however, that the increased melt viscosity of the nanocomposite sample does not significantly affect the filament processability, which means the FR PA6 nanocomposite was still found to be suitable for FFF printing.

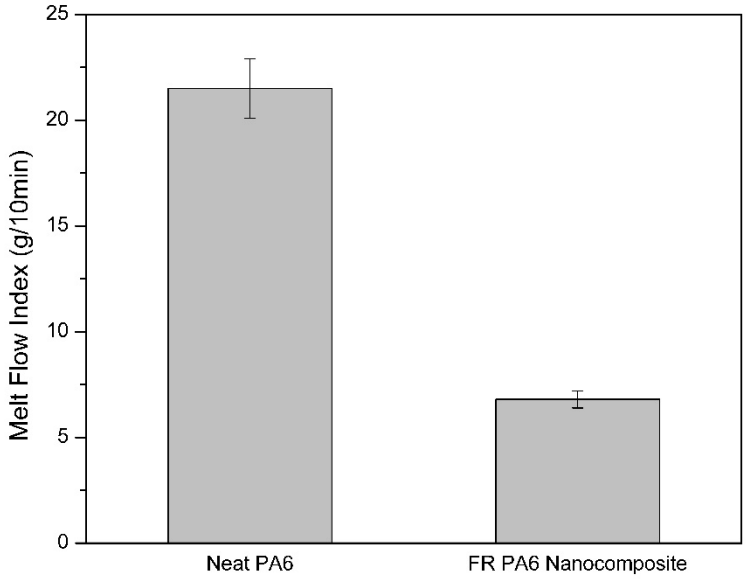


Figure 5 MFI comparison between neat PA6 and the FR PA6 nanocomposite.

3.2 TGA

Figure 5 shows the thermal degradation curves of the two formulations. The decomposition temperatures calculated from the thermographs are summarized in Table 3. The 10 wt% mass loss temperature for neat nylon 6 is 443 °C; after adding flame retardant, the 10 wt% mass loss temperature dropped ~18 °C which is identical to previous results [16]. The lower onset degradation temperature is common in polymer systems containing intumescent compounds [21, 22] and can be explained by the formation of phosphoric esters through the reaction between phosphate in the flame retardant and hydrocarbons in the nylon 6 [23]. At higher temperatures, the FR nanocomposites outperforms the neat PA6 as indicated by the higher 50 wt% mass loss temperature. After heating the materials to 1000 °C, neat nylon 6 samples have only 1wt% of

char residue left. The char residue increased significantly to over 9 wt% for the FR nanocomposite formulation. From the DrTGA results, neat nylon 6 has a single mass loss peak at 477 °C. Because the charring effect of the flame retardants, the mass loss peak for the flame-retardant-modified nanocomposite formulations show a slightly higher temperature at 479.4 °C.

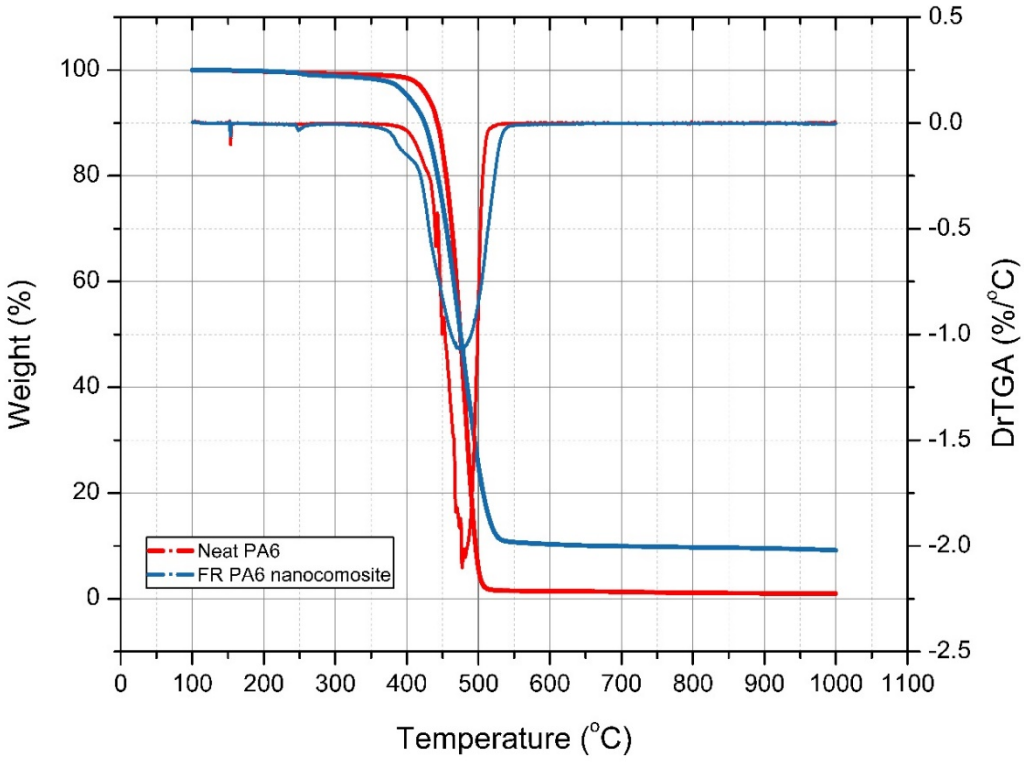


Figure 6 TGA and DrTGA curves of neat PA6 (red) and FR PA6 nanocomposite (blue).

Table 2 Summary of decomposition temperatures and residual mass

sample	**Tdec 10wt% (°C)**	**Tdec 50wt% (°C)**	**Peak mass loss temperature (°C)**	**Residual mass (wt%)**
neat PA6	443	475	477	1.0
FR PA6 nanocomposite	425	475	479	9.2

3.3 MCC

To compare the flammability between neat PA6 and the FR PA6 nanocomposite, representative heat release curves of both samples are shown in Figure 6. Heat Release Capacity (HRC) and total heat release of both samples are compared in Figure 7. Similar to TGA results, the FR PA6 nanocomposite formulation has lower onset degradation temperature than the neat PA6. The FR PA6 exhibited significantly reduced peak heat release rates, which is indicative of lower

flammability. This reduced Heat Release Capacity (HRC) was achieved by a combination of FR additive and the barrier effect from the nanoclay [16]. The total heat release of the nanocomposite sample is slightly lower than the unmodified PA6 due to the presence of FR additives and nanoclay (Figure 8).

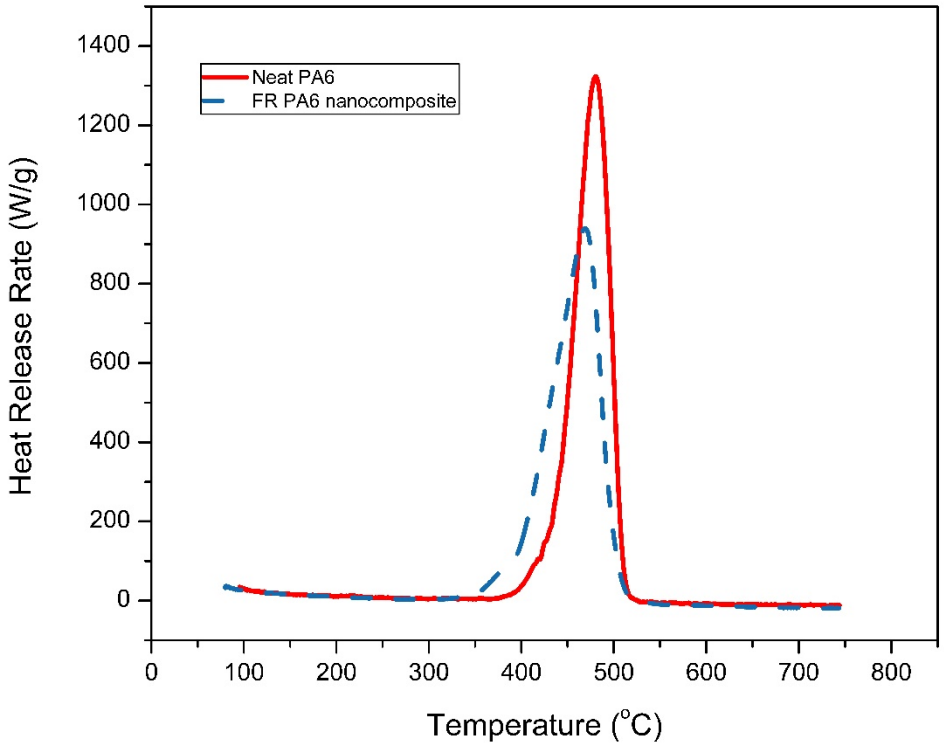


Figure 7 Representative MCC heat release curves of neat PA6 and FR PA6 nanocomposite

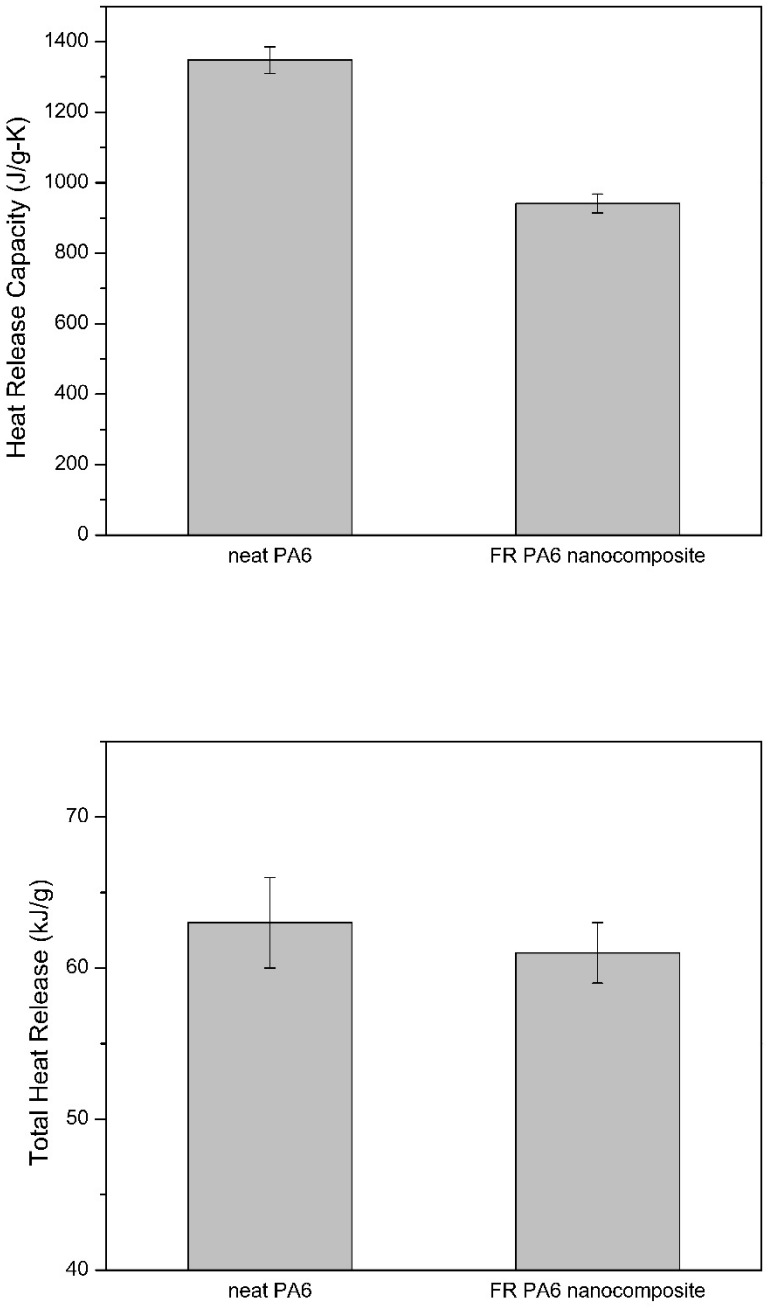
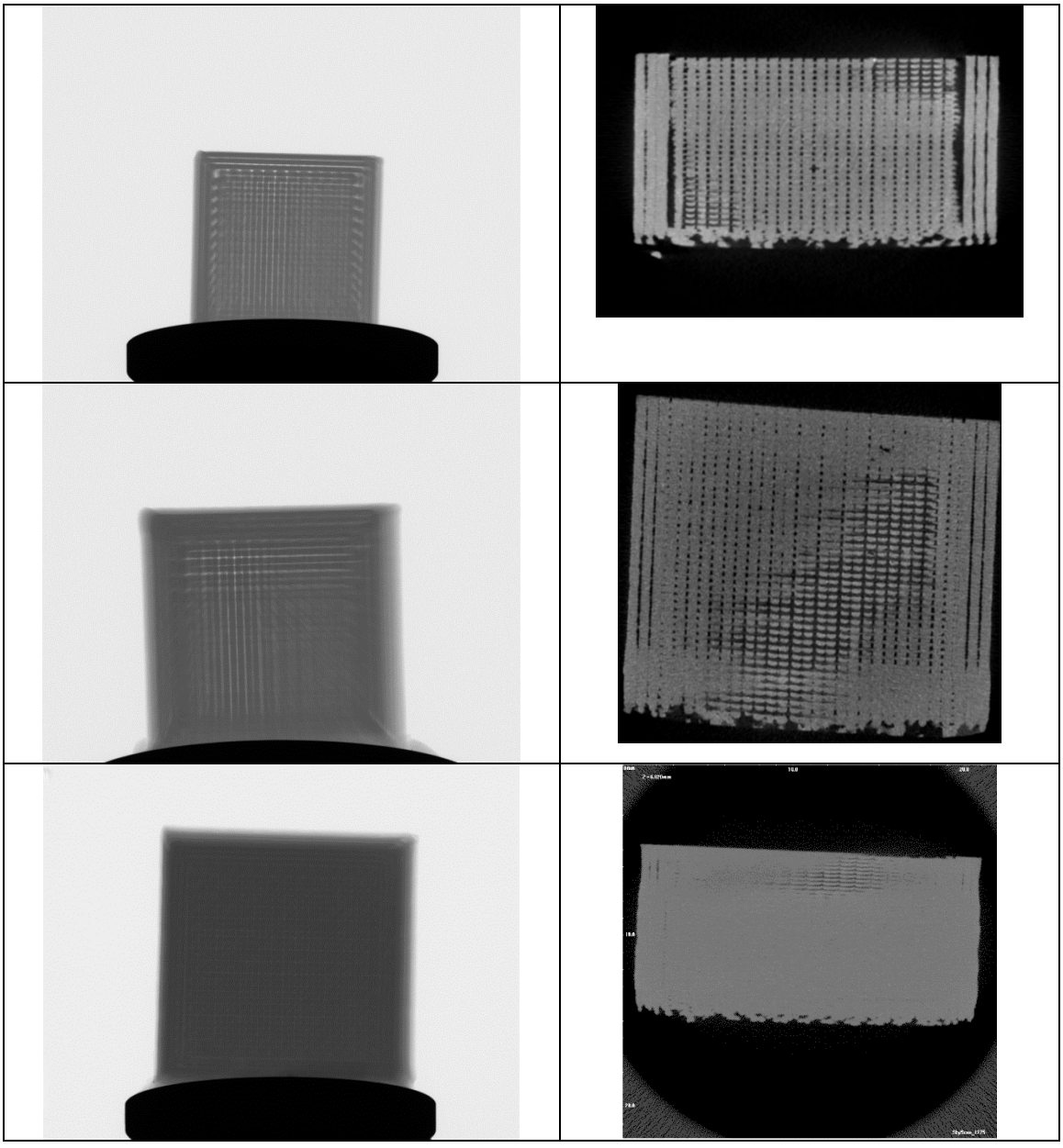


Figure 8 Comparison of HRC and total heat release from MCC results.

3.4 Micro-CT results

Extrusion multiplier (EM) can be defined as the amount of material coming out of the nozzle to build the printed cube. EM was controlled by changing the multiplier option in simplify3D. It can be observed in Figure 9 that both raw image and reconstructed micro-CT images are full of

porosity as evidenced from their repeated pattern for 0.95 EM. As to 0.98 EM in 2nd row in Figure 9, both porosity and the usual pattern from 0.95 EM were partially lost. Interestingly, use of 1.0 EM resulted in complete filling of pores and there was no visible pattern in the reconstructed image. These results indicated that the appropriate amount of material was extruded at EM 1.0 to build layer by layer the cube structure with low and reproducible porosity. Further increase by 5 % of EM value resulted increase in porosity which indicated that EM 1.0 is optimum print settings for the PA6 FR nanocomposite.



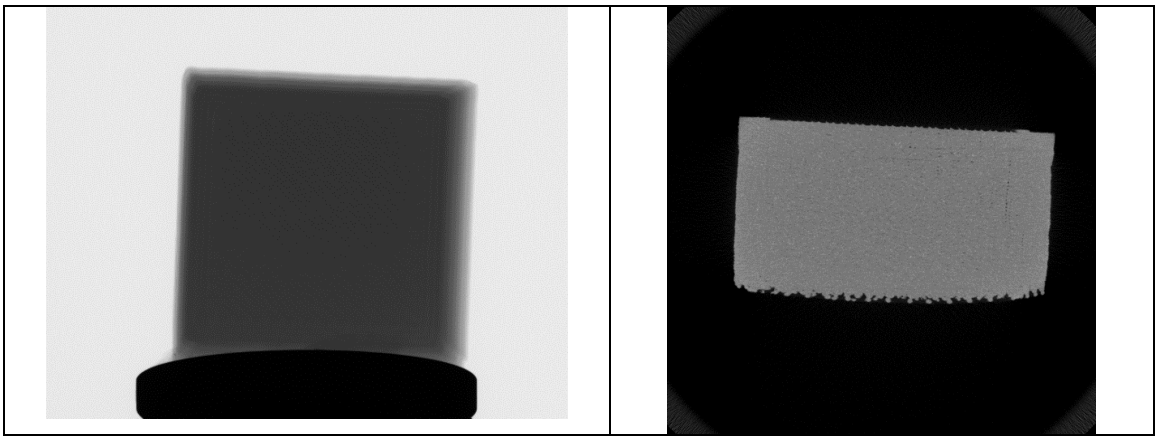


Figure 9 Representative Original (Left) and Reconstructed (Right) Micro-CT images of PA6 FR polymer. Row 1-4: 1(0.95 Multiplier), 2(0.98 Multiplier), 3 (1.0 Multiplier), 4 (1.05 Multiplier).

Open pores are classified as the property of the volume of interest (VOI) as they intersect the boundary of VOI. A 'closed pore' in contrast a group of black pixels that is fully surrounded by a border of white pixels. To calculate the porosity, a reasonable ROI was constructed on numerous reconstructed images using the CTan software. It can be seen from Table 6 that increase of multiplier from 0.95 to 1.0 resulted significant decrease in total porosity and total pore volumes. It is worth mentioning that open porosity was lowest for 1.05 extrusion multiplier (EM) whereas closed porosity was found lowest for 1 EM.

Table 3 Porosity results of PA6 FR printed Cubes

Properties	**0.95 Multiplier**	**0.98 Multiplier**	**1.0 Multiplier**	**1.05 Multiplier**
Open Porosity, %	80.13	46.97	1.20	0.10
Closed Porosity, %	0.058	0.53	0.10	2.22
Total Porosity, %	80.14	47.25	1.30	2.33
Total Pore Volume, mm^3	34.86	16.57	24.25	60.57

4. CONCLUSIONS

In summary, an optimized non-halogenated FR PA6 nanocomposite with combination of non-halogenated flame retardant, thermoplastic elastomer, and nanoclay was successfully compounded and extruded into FFF compatible filaments. The addition of various fillers increased the melt viscosity as indicated by the lower MFI value. Both TGA and MCC results from the FR formulation show improved thermal and flammability as compared to the neat PA6. The lower onset degradation temperature was caused by the FR additive. Micro-CT provides a convenient way of analysis to optimize the print conductions for reproducible microstructure and porosity. With such optimization, it is possible to control sample preparation so that the

flammability results can be compared with confidence. CT scans showed that extrusion multiplier lower or higher than 1.0 results in higher porosity thus the printing extrusion multiplier of 1.0 is recommended for optimal print quality.

5. REFERENCES

[1] ASTM. Standard Terminology for Additive Manufacturing – General Principles – Terminology. ASTM ISO/ASTM52900-15. West Conshohocken, PA2015.

[2] Ngo TD, Kashani A, Imbalzano G, Nguyen KTQ, Hui D. Additive manufacturing (3D printing): A review of materials, methods, applications and challenges. Composites Part B: Engineering. 2018;143:172-96.

[3] Küpper D, Heising W, Corman G, Wolfgang M, Knizek C, Lukic VJD, Boston Consulting Group. Get ready for industrialized additive manufacturing. 2017.

[4] Richardson MJ, Wu H, Wilcox TJ, Broaddus M, Lin PC, Krifa M, et al. Flame Retardant Nylon 6 Nanocomposites for Fused Deposition Modelling (FDM) Applications. SAMPE 2017. Seattle2017.

[5] Wang X, Jiang M, Zhou Z, Gou J, Hui D. 3D printing of polymer matrix composites: A review and prospective. Composites Part B: Engineering. 2017;110:442-58.

[6] Ertay DS, Yuen A, Altintas Y. Synchronized material deposition rate control with path velocity on fused filament fabrication machines. Additive Manufacturing. 2018;19:205-13.

[7] Blum A, Ames BN. Flame-retardant additives as possible cancer hazards. Science. 1977;195:17-23.

[8] Mark HF, Kroschwitz JI. Encyclopedia of polymer science and engineering: Wiley; 1986.

[9] Chen Y, Fang Z, Yang C, Wang Y, Guo Z, Zhang Y. Effect of clay dispersion on the synergism between clay and intumescent flame retardants in polystyrene. Journal of Applied Polymer Science. 2010;115:777-83.

[10] Wu H, Krifa M, Koo JH. Flame retardant polyamide 6/nanoclay/intumescent nanocomposite fibers through electrospinning. Textile Research Journal. 2014.

[11] Weil ED, Levchik S. Current Practice and Recent Commercial Developments in Flame Retardancy of Polyamides. Journal of Fire Sciences. 2004;22:251-64.

[12] Wu H, Koo J, Krifa M. Flame Retardant Polyamide 6 Elastomer Blends Processing and Characterization. SAMPE Conference Proceedings. Seattle, WA2014.

[13] Wu H, Koo J, Krifa M. Rubber Toughening of Flame Retardant Polyamide 6 Nanocomposite Systems. SAMPE Conference Proceedings. Dallas, TX2015.

[14] Wu H. Flame retardant nylon 6 nanocomposite fibers: processing and characterization: The University of Texas at Austin; 2016.

[15] Wu H, Krifa M, Koo JH. Rubber (SEBS-G-MA) Toughened Flame Retardant Polyamide 6: Microstructure, Combustion, Extension, and Izod Impact Behavior. Polymer-Plastics Technology and Engineering. 2017.

[16] Wu H, Ortiz R, Correa Renan De A, Krifa M, Koo Joseph H. Self-Extinguishing and Non-Drip Flame Retardant Polyamide 6 Nanocomposite: Mechanical, Thermal, and Combustion Behavior. Flame Retardancy and Thermal Stability of Materials2018. p. 1.

[17] Braun U, Schartel B, Fichera MA, Jäger C. Flame retardancy mechanisms of aluminium phosphinate in combination with melamine polyphosphate and zinc borate in glass-fibre reinforced polyamide 6,6. Polymer Degradation and Stability. 2007;92:1528-45.

[18] Doğan M, Bayramlı E. The flame retardant effect of aluminum phosphinate in combination with zinc borate, borophosphate, and nanoclay in polyamide-6. Fire and Materials. 2014;38:92-9.
[19] Laura DM, Keskkula H, Barlow JW, Paul DR. Effect of rubber particle size and rubber type on the mechanical properties of glass fiber reinforced, rubber-toughened nylon 6. Polymer. 2003;44:3347-61.
[20] Dul S, Fambri L, Pegoretti A. Filaments production and fused deposition modelling of ABS/carbon nanotubes composites. Nanomaterials. 2018;8:49.
[21] Wu H, Yin X, Krifa M, Londa M, Koo J. Fabrication and Characterization of Flame Retardant Polyamide 6 Nanocomposites via Electrospinning. SAMPE TECH 2011. Fort Worth, TX2011.
[22] Bourbigot S, Duquesne S. Fire retardant polymers: recent developments and opportunities. Journal of Materials Chemistry. 2007;17:2283-300.
[23] Peng H-Q, Zhou Q, Wang D-Y, Chen L, Wang Y-Z. A novel charring agent containing caged bicyclic phosphate and its application in intumescent flame retardant polypropylene systems. Journal of Industrial and Engineering Chemistry. 2008;14:589-95.